



Supplementary Information

Mesoscopic Modeling of Encapsulation of Capsaicin by Lecithin/Chitosan Liposomal Nanoparticles

Ketzasmin A. Terrón-Mejía ^{1,2}, Evelin Martínez-Benavidez ¹, Inocencio Higuera-Ciapara ¹, Claudia Virués ³, Javier Hernández ⁴, Zaira Domínguez ⁴, W. Argüelles-Monal ⁵, Francisco M. Goycoolea ⁶, Roberto López-Rendón ^{7*}, and Armando Gama Goicochea ^{8*}

¹ Centro de Investigación y Asistencia en Tecnología y Diseño del Estado de Jalisco, A.C., Av. Normalistas 800, Colinas de la Normal, Guadalajara, Jalisco, 44270, México; (K.A.T.-M. : ket.a.t.m@gmail.com), (E.M.-B. : emartinez@ciatej.mx), (I.H.-C. : inohiguera@ciatej.mx)

² Instituto Tecnológico Superior de Zongolica, Km. 4 Carretera a la Compañía, Zongolica, Veracruz, 95005, México; (K.A.T.-M. : ket.a.t.m@gmail.com)

³ Centro de Investigación y Asistencia en Tecnología y Diseño del Estado de Jalisco, A.C., Clúster Científico y Tecnológico Biomimic®, Carretera antigua a Coatepec No. 351, Colonia El Haya, Xalapa, Veracruz 91070, México; (cvirues@ciatej.mx)

⁴ Unidad de Servicios de Apoyo en Resolución Analítica, Universidad Veracruzana, Apartado Postal 575, Xalapa, Veracruz, 91190, México; (J.H. : javmartinez@uv.mx), (Z.D. : zdominguez@uv.mx)

⁵ Centro de Investigación en Alimentación y Desarrollo A. C., Grupo de Investigación en Biopolímeros, Carr. a La Victoria km. 0.6, Hermosillo, Sonora, 83304, México; waldo@ciad.mx

⁶ School of Food Science and Nutrition. University of Leeds. Woodhouse Ln, Leeds LS2 9JT, United Kingdom; F.M.Goycoolea@leeds.ac.uk

⁷ Laboratorio de Bioingeniería Molecular a Multiescala, Facultad de Ciencias, Universidad Autónoma del Estado de México, Av. Instituto Literario 100, Toluca, Estado de México, 50000, México; roberto.lopez.rendon@gmail.com

⁸ División de Ingeniería Química y Bioquímica, Tecnológico de Estudios Superiores de Ecatepec, Av. Tecnológico s/n, Ecatepec, Estado de México, 55210, México; agama@alumni.stanford.edu

* Correspondence: roberto.lopez.rendon@gmail.com; agama@alumni.stanford.edu; Tel.: +52-555-000-2300, and +52-722-296-5554

Received: date; Accepted: date; Published: date

Keywords: capsaicin; chitosan; lecithin; dissipative particle dynamics

I. METHODOLOGY, MODELS AND COMPUTATIONAL DETAILS

A. Dissipative particle dynamics simulation (DPD)

Some years ago Hoogerbrugge and Koelman [1] introduced a new simulation technique called dissipative particle dynamics (DPD). It is based on the simulation of soft spheres (“beads”), whose motion is governed by simple force laws; in addition, it allows for the mesoscopic-scale modeling of the self-assembly of surfactant and polymer systems. DPD is based on a coarse-grained representation, where the internal degrees of freedom of the molecules are integrated out in favour of a less atomistically detailed and more mesoscopic description of the system. Beads interact through soft, short range potentials that lead to improved computational efficiency. Despite the simplicity of the models, DPD can provide quantitatively and qualitatively correct descriptions of structural and thermodynamic properties of complex systems [2, 3].

DPD is an approach based on the classical equations of motion, DPD has enjoyed enormous popularity in the modeling of systems at mesoscopic scale. DPD is a coarse-grained simulation method in which a complex molecule, such as nanoliposomes, is represented by soft spherical beads

45 joined with springs. The interaction is usually described through simple and pairwise-additive
 46 potentials. Similarly, to molecular dynamics simulations, particle positions and velocities in DPD are
 47 governed by the Newtonian law of motion:

$$48 \frac{d\mathbf{r}_i}{dt} = \mathbf{v}_i, \quad m_i \frac{d\mathbf{v}_i}{dt} = \mathbf{F}_i, \quad (S1)$$

50 where \mathbf{r}_i , \mathbf{v}_i and m_i are the position, velocity and mass of the i th bead, respectively, and \mathbf{F}_i is the
 51 total force exerted upon it. The total force is the sum of the conservative force (\mathbf{F}^C), random force (\mathbf{F}^R),
 52 and dissipative force (\mathbf{F}^D) as follow:

$$53 \mathbf{F}_{ij} = \sum_{i \neq j}^N [\mathbf{F}^C(\mathbf{r}_{ij}) + \mathbf{F}^R(\mathbf{r}_{ij}) + \mathbf{F}^D(\mathbf{r}_{ij})] \quad (S2)$$

54 The conservative force between the i th particle and the j th particle determines the thermodynamics
 55 of the DPD system and is defined by a soft repulsion:

$$56 \mathbf{F}_{ij}^C = \begin{cases} a_{ij}(1 - r_{ij})\hat{\mathbf{r}}_{ij} & r_{ij} \leq r_c \\ \mathbf{0} & r_{ij} > r_c \end{cases} \quad (S3)$$

57 where a_{ij} is the parameter expressing the maximum repulsion between i th and the j th beads, and
 58 $\mathbf{r}_{ij} = \mathbf{r}_i - \mathbf{r}_j$, $r_{ij} = |\mathbf{r}_{ij}|$, $\hat{\mathbf{r}}_{ij} = \mathbf{r}_{ij}/r_{ij}$ is the unit vector denoting the direction from bead i to j . r_c is a
 59 cut-off radius, and it gives the extent of the interaction range between a pair of beads. The other two
 60 forces in Eq. (S2) are the random force (\mathbf{F}^R), which is given as follows:

$$61 \mathbf{F}_{ij}^R = \sigma \omega^R(r_{ij}) \xi_{ij} \hat{\mathbf{r}}_{ij} \quad (S4)$$

62 and the dissipative force (\mathbf{F}^D):

$$63 \mathbf{F}_{ij}^D = -\gamma \omega^D(r_{ij}) [\mathbf{r}_{ij} \cdot \mathbf{v}_{ij}] \hat{\mathbf{r}}_{ij} \quad (S5)$$

64 In Eq. (S4), σ is the amplitude of the noise. ξ_{ij} is a random number between 0 and 1 and is subject to
 65 a uniform distribution for simplicity; it is statistically independent from the pair of beads. In Eq. (S5),
 66 $\mathbf{v}_{ij} = \mathbf{v}_i - \mathbf{v}_j$ is the difference between the velocity of the i th bead and the j th bead, γ is the friction
 67 coefficient. The ω^R and ω^D are weight functions; the combination of the dissipative and random
 68 forces leads to a thermostat that conserves the total momentum of the system. The magnitude of the
 69 dissipative and stochastic forces are related through the fluctuation–dissipation theorem [4]:

$$70 \omega^D(r_{ij}) = [\omega^R(r_{ij})]^2 = \max \left\{ \left(1 - \frac{r_{ij}}{r_c}\right)^2, \mathbf{0} \right\} \quad (S6)$$

71 where r_c is a cut-off distance. At interparticle distances larger than r_c , all forces are equal to zero.
 72 This simple distance dependence of the forces, which is a good approximation to the one obtained by
 73 spatially averaging a van der Waals–type interaction, allows one to use relatively large integration
 74 time steps. The strengths of the dissipative and random forces are related in a way that keeps the
 75 temperature internally fixed, $k_B T = \frac{\sigma^2}{2\gamma}$; k_B being Boltzmann's constant and T the temperature. The
 76 natural probability distribution function of the DPD model is that of the canonical ensemble, where
 77 N (the total particle number), V (Volume), and T (Temperature) are kept constant. The equations of
 78 motion are solved using the velocity Verlet algorithm adapted to DPD [5].

79 In this work, both the chains of the chitosan polymer and the molecules of lecithin and capsaicin are
 80 connected by a harmonic spring as follows

$$81 \mathbf{F}_{ij}^S = -k_s(\mathbf{r}_{ij} - \mathbf{r}_0)\hat{\mathbf{r}}_{ij} \quad (S7)$$

82 Where the spring constant is k_s and the equilibrium distance is r_0 [6]. Using the same harmonic
83 model, we control the angle between every three beads and the equation for this type of bond is

$$84 \quad \mathbf{F}_{ijk}^\theta = -k_\theta(\theta_{ijk} - \theta_0)\hat{\mathbf{b}}_{ijk} \quad (S8)$$

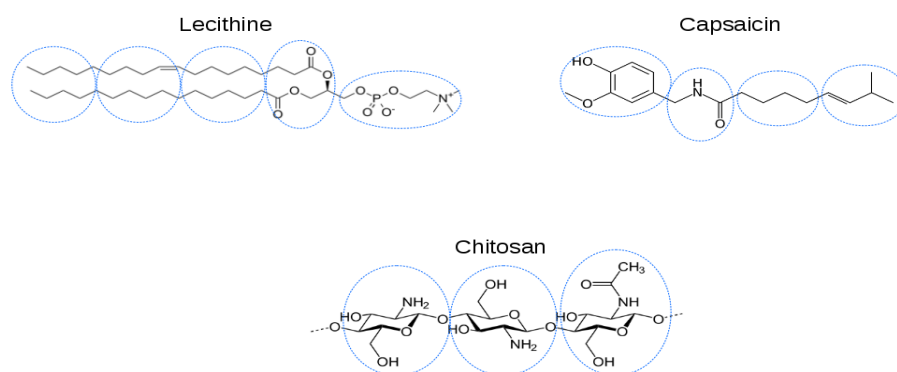
85 Where k_θ is the spring constant, θ_{ijk} is the angle between i - j - k particles and θ_0 is the equilibrium
86 angle. For simplicity, conservative interaction parameters for each one components are listed in Table
87 S1. The interaction parameters have been obtained using the group contribution method [7] based on
88 the solubility of each bead and following the standard technique for parametrizing the DPD
89 interactions [8].

90 Finally, two fundamental properties were used namely, the radial distribution function, $g(\mathbf{r})$, and
91 the potential mean force (PMF), $W_{PMF}(\mathbf{r})$. We focus here on the latter, which is an effective pair
92 interaction that provides important thermodynamic information about many – body systems. It can
93 be obtained from the radial distribution functions, $g(\mathbf{r})$, through the relation [9]:

$$94 \quad W_{PMF}(r) = -k_B T \ln[g(r)] \quad (S9)$$

95 A. Models

96 The exact division of capsaicin, lecithin and chitosan molecules is presented in next figure S1.



97

98 **Figure S1. (Color online).** Construction of beads in every molecule.

99 The matrix of interaction parameters a_{ij} according to Eq. S3 between every group shown in figure
100 S1 is presented in the next table.

101 **Table S1.** Interaction matrix a_{ij} . The labels in this table are according to the description of figure 1 of
102 the original article.

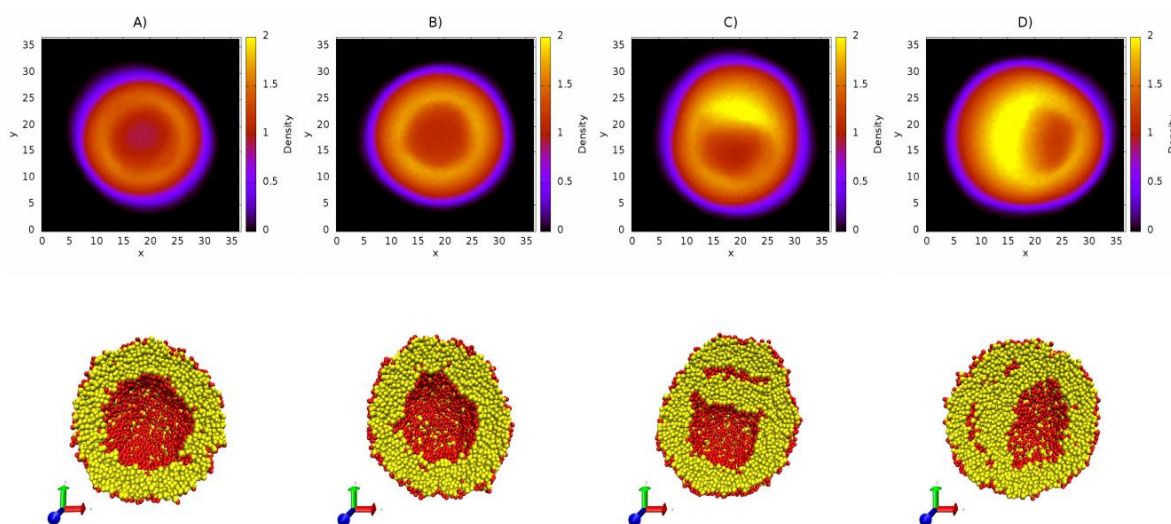
	L1	L2	L3	A	G	C1	C2	C3	W
L1	78.33								
L2	80.25	78.33							
L3	95.21	85.85	78.33						
A	80.67	85.72	103.82	78.33					

G	82.05	87.15	103.43	78.68	78.33				
C1	78.34	79.51	89.85	80.89	82.35	78.33			
C2	89.20	93.48	103.95	84.73	83.14	89.50	78.33		
C3	85.72	81.48	78.34	93.79	98.29	85.35	103.47	78.33	
W	89.25	92.79	101.21	83.41	80.98	89.49	78.62	100.83	78.33

103 Parameters of the intramolecular forces are shown follows; the corresponding parameters of bonding
 104 forces are: for all molecules $r_0 = 0.7$ and $k_s = 100$ [6]. Parameters corresponding to binding forces
 105 are for lecithin molecules are $\theta_0 = 170.0$ and $k_\theta = 50.0$. For chitosan are $\theta_0 = 118.5.0$ and $k_\theta =$
 106 10.0 , finally for capsaicin are $\theta_0 = 175.0$ and $k_\theta = 10.0$. The angles θ_0 are taken of molecular
 107 structures, from representative atoms in every coarse-graining group.

108 Others details of our simulations are $k_B T = 1.0$, time step $\Delta t = 0.03$, mass $m = 1.0$ and $r_c = 1.0$.
 109 The parameters σ y γ of random and dissipative forces are equal to 3.0 and 4.5 respectively. All
 110 simulations performed 50 blocks of 1×10^5 steps to reach a total of 5×10^6 steps or 24 μ s. The
 111 density of all systems are chose as 3.0 and the total number of particles in each simulation is 150000.
 112 All simulation parameters are in DPD units.

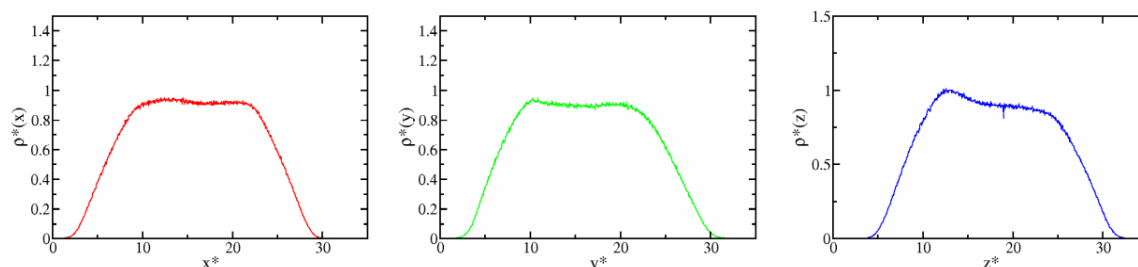
113 For fix the number of lecithin molecules that made a nanoliposome, we run an extra set of
 114 simulations, these simulations consist in change the concentration of lecithin molecules in the
 115 liposome structure. The chosen concentrations were: $\chi_{LC} = 0.48, 0.60, 0.73, \text{ and } 0.85 \text{ M}$, where
 116 the LC subscript refers to lecithin molecules. Density maps of these simulations shown is figure S2.



117
 118 **Figure S2. (Color online). Initial configuration of nanoliposome.** A snapshot of the initial
 119 configuration Density maps of lecithin at different concentrations. A) 3929 lecithin molecules $\chi_{LC} =$
 120 0.48 M . B) 4929 lecithin molecules $\chi_{LC} = 0.60 \text{ M}$. C) 5929 lecithin molecules $\chi_{LC} = 0.73 \text{ M}$. D) 6929
 121 lecithin molecules $\chi_{LC} = 0.85 \text{ M}$.

122 We use these results for choose the ideal concentration of lecithin. The concentration chosen is $\chi_{LC} =$
 123 0.60 M , the reason is because in the case A) the density of lecithin is low and there is a risk of the
 124 membrane breaking and in cases C) and D) the density of lecithin is very high such that the aqueous
 125 core is smaller and the structure of liposome is deformed.

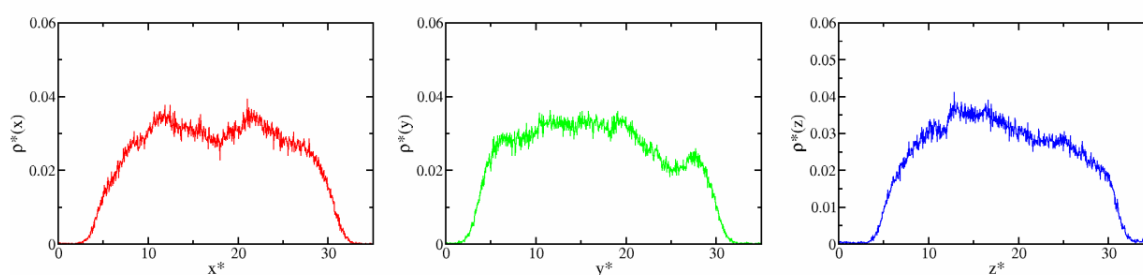
126 The density profiles of capsaicin and lecithin help us to estimate the mean size of nanoliposome and
 127 the encapsulation efficiency. In the figure S3 we show the density profiles only for the case of $\chi_{CS} =$
 128 6mM and $\chi_{CP} = 30$ mM. The way to obtain these properties is to taken the average of density profile
 129 in the x , y and z coordinates and measure when the density begins to increase and when the density
 130 newly is close to zero and compute the difference. This difference is taken as mean size of
 131 nanoliposome.



132

133 **Figure S3. (Color online).** Density profiles of lecithin in the coordinates x (red), y (green) and z (blue)
 134 starting in left to right

135 For the efficiency of encapsulation is need to integrate a density profile of capsaicin for obtain the
 136 number of molecules inside the nanoliposome and applicate the equation of encapsulation efficiency
 137 (EE). See the discussion in the main text about the calculation of the EE. Density profiles of capsaicin
 138 is shown in the figure S4.



139

140 **Figure S4. (Color online).** Density profiles of capsaicin in the coordinates x (red), y (green) and z (blue)
 141 starting in left to right.

142 References

- 143 1. Hoogerbrugge, P.J.; Koelman, J.M.V.A. Simulating microscopic hydrodynamic phenomena with
 144 dissipative particle dynamics. *Europhys. Lett.* **1992**, *19*, 155-160. <https://doi.org/10.1209/0295-5075/19/3/001>.
- 145 2. Murtola, T.; Karttunen, M.; Vattulainen, I. Systematic coarse graining from structure using internal states:
 146 Application to phospholipid/cholesterol bilayer. *J. Chem. Phys.* **2009**, *131*, 08B601.
 147 <https://doi.org/10.1063/1.3167405>.
- 148 3. Balderas Altamirano, .M.A.; Pérez, E.; Gama Goicochea, A. On Finite Size Effects, Ensemble Choice and
 149 Force Influence in Dissipative Particle Dynamics Simulations. C.J. Barrios Hernández et al. (Eds.): CARLA
 150 2016, CCIS 697, High Performance Computing (pp. 314–328), Springer International Publishing.
- 151 4. Español, P.; Warren, P. Statistical mechanics of dissipative particle dynamics. *Europhys. Lett.* **1995**, *30*, 191–
 152 196. <https://doi.org/10.1209/0295-5075/30/4/001>.
- 153 5. Vattulainen, I.; Karttunen, M.; Besold, G.; Polson, J.M. Integration schemes for dissipative particle dynamics
 154 simulations: From softly interacting systems towards hybrid models. *J. Chem. Phys.* **2002**, *116*, 3967–3979.
 155 <https://doi.org/10.1063/1.1450554>.
- 156 6. Gama Goicochea, A.; Romero-Bastida, M.; López-Rendón, R. Dependence of thermodynamic properties of
 157 model systems on some dissipative particle dynamics parameters. *Mol. Phys.* **2007**, *105*, 2375–2381.
 158 <https://doi.org/10.1080/00268970701624679>.

- 159 7. Ravindra, R.; Krovvidi, K.R.; Khan, A.A. *Carbohydr. Polym.* **1998**, *36*, 121–127. <https://doi.org/10.1016/S0144->
160 8617(98)00020-4.
- 161 8. Groot, R.B.; Warren, P.B. *J. Chem. Phys.* **1997**, *107*, 4423–4435. <https://doi.org/10.1063/1.474784>.
- 162 9. Roux, B. The calculation of the potential of mean force using computer simulations. *Comp. Phys. Comm.*
163 **1995**, *91*, 275–282. [https://doi.org/10.1016/0010-4655\(95\)00053-I](https://doi.org/10.1016/0010-4655(95)00053-I).
- 164



© 2018 by the authors. Submitted for possible open access publication under the terms and conditions of the Creative Commons Attribution (CC BY) license (<http://creativecommons.org/licenses/by/4.0/>).